OPTIMAL TEMPERATURE RANGE FOR DETERMINING MAGNETOCALORIC MAGNITUDES FROM HEAT CAPACITY

L.M. Moreno-Ramírez [a], J.S. Blázquez [a], J.Y. Law [a], V. Franco [a], A. Conde [a]

[a] Dpto. Física de la Materia Condensada, ICMSE-CSIC, Universidad de Sevilla, P.O. Box 1065, 41080-Sevilla, Spain

ABSTRACT

The determination of the magnetocaloric magnitudes (specific magnetic entropy change, Δs_M, and adiabatic temperature change, ΔT_{ad}) from heat capacity (c_H) measurements requires measurements performed at very low temperatures (~0 K) or data extrapolation when the low temperature range is unavailable. In this work we analyze the influence on the calculated Δs_M and ΔT_{ad} of the usually employed linear extrapolation of c_H from the initial measured temperature down to 0 K. Numerical simulations have been performed using the Brillouin equation of state, the Debye model and the Fermi electron statistics to reproduce the magnetic, lattice and electronic subsystems, respectively. It is demonstrated that is not necessary to reach experimentally temperatures very close to 0 K due to the existence of certain starting temperatures of the experiments, the same for Δs_M and ΔT_{ad}, that minimize the error of the results. A procedure is proposed to obtain the experimental magnitudes of Δs_M and ΔT_{ad} with a minimum error from c_H data limited in temperature. It has been successfully applied to a GdZn alloy after comparing with results derived from magnetization measurements.

1. INTRODUCTION

The application of a magnetic field in adiabatic conditions to a magnetic material causes a variation of the sample temperature (ΔT_{ad}) due to the coupling between the lattice and magnetic subsystems. This effect is known as the magnetocaloric effect (MCE) [1,2]. Alternatively, the MCE can be quantified as the specific magnetic entropy change (Δs_M) during the variation of an applied magnetic field in an isothermal process. This effect was widely used to achieve ultralow temperatures (below 1 K) making use of paramagnetic salts [3]. Nowadays, the interest on MCE is increasing due to the possibility to perform magnetic refrigerators at room temperature. This technology has been shown as an energy efficient and environmental friendly (due to the absence of gasses responsible for greenhouse effect and ozone depletion) alternative to the conventional systems [4,5].

In order to optimize the material performances to be applied in a refrigerator device, a basic step is an accurate characterization of the magnetocaloric magnitudes. In isothermal conditions, the Δs_M for a magnetic field change ΔH is obtained using the Maxwell relations [6] as:

$$\Delta s_M(T, \Delta H) = \mu_0 \int_{H_I}^{H_F} \left(\frac{\partial \sigma}{\partial T}\right)_H \mathrm{d}H \qquad (1)$$

where H_I and H_F are the initial and final magnetic fields, respectively, T is the temperature, σ is the specific magnetization and μ_0 is the magnetic permeability of the vacuum (in this work, equations and magnitudes are expressed in the SI).

On other hand, making use of the definition of the specific heat capacity at constant magnetic field (c_H) and taking into the Maxwell relations and the adiabatic condition, ΔT_{ad} can be obtained as:

$$\Delta T_{ad}(T, \Delta H) = -\mu_0 \int_{H_I}^{H_F} \frac{T}{c_H} \left(\frac{\partial \sigma}{\partial T}\right)_H \mathrm{d}H. \quad (2)$$

From equations (1) and (2) it can be deduced that the MCE is maximum when there is an abrupt change in magnetization with respect to the temperature, i.e. in the region close to a magnetic transition.

Previous expression require the acquisition of magnetization data as a function of temperature and field, for Δs_M, and besides this, c_H measurements as a function of temperature and field for determining ΔT_{ad}. On the other hand, the two fundamental magnetocaloric magnitudes, can be obtained using only calorimetric data [7,8]. For a constant magnetic field, the specific total entropy of the system (s_H) can be obtained from heat capacity data through:

$$s_H(T) = \int_0^T \frac{c_H}{T} \mathrm{d}T + s_{0\,K,H} \quad (3)$$

where $s_{0\,K,H}$ is the entropy at 0 K for a magnetic field H. Δs_M and ΔT_{ad} are obtained from equation (3) as:

$$\Delta s_M(T, \Delta H) = [s_{H_F}(T) - s_{H_I}(T)]_T \quad (4)$$

$$\Delta T_{ad}(T, \Delta H) = [T_{H_F}(s) - T_{H_I}(s)]_s \quad (5)$$

where in order to calculate ΔT_{ad}, the entropy curves $s_H(T)$ have to be inverted as $T_H(s)$.

In both cases, equations (1 and 2) and equations (4 and 5), the heat capacity measurements are needed to obtain ΔT_{ad}, although in the first case, it is also necessary to have the magnetization data and, in the second case, we have to be able to calculate $s_{0\,K,H}$ and to reach temperatures close to 0 K (see equation (3)).

Concerning the calculus of the MCE from calorimetric measurements, the $s_{0\,K,H}$ term would not affect Δs_M if it is assumed that, in a condensed system, it is field independent.

However, for ΔT_{ad}, its contribution is not zero but it is assumed small [7], and usually this term is neglected in the calculus of both magnitudes. In the case that temperatures close to 0 K could not be reached, the approximated calculus will be considerably affected (some kind of assumption must be done for the missing data range, e.g. a linear behavior of c_H). The experimental limitations can be ascribed to limitations of the experimental setup (e.g. the sample is cooled down using liquid N_2) or to the difficulties to measure c_H in a large temperature range (e.g. due to stability limitations of the grease usually employed to attach the sample to the calorimetric chip).

In the present work, the influence of assuming a linear behavior of the heat capacity from the initial temperature measured down to 0 K (assuming c_H(0 K)=0) on the calculated magnetocaloric magnitudes will be discussed. Numerical simulations have been performed using the Brillouin equation of state, the Debye model and the Fermi electron statistics to reproduce the magnetic, lattice and electronic subsystems, respectively. The obtained results from the simulations allow us to propose a procedure to minimize the associated error in experimental Δs_M and ΔT_{ad} data. In order to check the validity of the proposed procedure, it has been applied to a single phase GdZn alloy. The results are compared to calculations derived from magnetization data.

2. EXPERIMENTAL TECHNIQUES AND MODELS

For both experimental data as well as for numerical simulations, the total entropy of the system has been numerically calculated from heat capacity data approximating equation (3) as [7]:

$$s_H^{ap}(T) = \frac{1}{2} c_H(T_{ini}) + \int_{T_{ini}}^{T} \frac{c_H}{T} \mathrm{d}T \qquad (6)$$

Where s_H^{ap} is the approximated entropy at a constant magnetic field (the superscript 'ap' will also denote the different magnitudes calculated from this data), c_H was measured at constant magnetic field, with T_{ini} as the initial temperature and the zero temperature entropy is not considered. In this expression, it is assumed a linear extrapolation from T_{ini} down to 0 K for c_H (assuming c_H(0 K)=0) as proposed by Pecharsky et al. [7] for measurements close to 0 K.

Theoretically, the heat capacity of the magnetic material can be expressed as the sum of the magnetic, lattice and electronic subsystems contributions. To simulate the magnetic subsystem, the Brillouin equation of state has been considered [9], where the heat capacity of the magnetic subsystem (C_M) is calculated according to [10]:

$$C_M = N_m K_B T \left(\partial \left[ln \left(\frac{\sinh\left(\frac{2J+1}{2J}x\right)}{\sinh\left(\frac{1}{2J}x\right)} \right) - xB_J(x) \right] \Big/ \partial T \right)_H \quad (7)$$

where $B_J(x)$ is the Brillouin function, $x=\mu_0 g \mu_B J H^*/k_B T$, H^* is the total field (considered as the applied magnetic field plus the molecular field), g is the spectroscopic splitting factor, μ_B is the Bohr magneton, J is the total angular momentum quantum number and N_m is the number of magnetic atoms. Although the Brillouin equation of state is a mean field approximation that does not predict the correct critical exponents for certain materials and it also presents some limitations at low temperatures due to not consider spin waves. Nevertheless, it is profusely used as a simple model for the simulation of magnetocaloric materials and, as it will be argued below, these mentioned limitations do not affect the main conclusions of this work: the existence of an optimal initial temperature for the lower limit of integration of c_H (T_{ini}^{opt}) and the procedure to identify it from experimental measurements. It has to be noted that the use of different

thermomagnetic equations of state will produce different values of T_{ini}^{opt}.The lattice contribution (C_l) has been considered assuming the Debye model for which [9]:

$$C_l = 9Nk_B\left(\frac{T}{\theta_D}\right)^3 \int_0^{\frac{\theta_D}{T}} \frac{x^4 e^x}{(e^x-1)^2}\,\mathrm{d}x \quad (8)$$

where N is the number of particles, k_B is the Boltzmann constant and θ_D is the Debye temperature.

For the electronic subsystem, the Fermi-Dirac statistics [9] gives for the heat capacity (Ce):

$$C_e = \frac{2}{3}\pi^2 {k_B}^2 V D(E_F) T \approx \gamma T \quad (9)$$

where V is the molar volume and $D(E_F)$ is the electron density of states at the Fermi level E_F. Gadolinium has been considered as the model material for the simulations as it is the well-known reference magnetocaloric material for room temperature applications with a ferro-paramagnetic transition, for which the main parameters are J=7/2, T_C=293 K, θ_D=163 K and γ=6.4 mJ mol^{-1} K^{-2} [11].

The single phase GdZn alloy was prepared by induction melting. Its structural and magnetic characterization can be found in [12]. GdZn presents the advantages of a simpler magnetic transition than pure Gd (with a spin reorientation transition close to the ferro-paramangetic transition [13,14]). Moreover, Gd behavior can be easily modified by impurities [15] and it is easily oxidated, while GdZn does not present such problems.The heat capacity and magnetization curves have been performed in a commercial Physical Property Measurement System from Quantum Design in the temperature range of 200–400 K for magnetic fields up to 2 T.

3. RESULTS AND DISCUSSIONS

3.1 SIMULATIONS

The simulated specific heat capacity (c_H) data of Gd at various magnetic fields are presented in figure 1. Using these data, the specific total entropy of the system (s_H) was calculated (inset of figure 1) according to equation (6) from 0 K. Figure 2 shows the calculated specific magnetic entropy change curves (Δs_M^{ap}) for $\mu_0 \Delta H$=2 T (H_I=0 in this work) using equation (6) starting from differentinitial temperatures (T_{ini}). It is observed that each curve differs from the curve starting integration at 0 K (denoted as *complete curve* from now) in a constant value which depends on the magnetic field change. As the initial temperature of integration increases, it can be observed that a non-monotonous tendency exists. The inset of figure 2 shows the differences of the peak between the approximated magnetic entropy change curve^p ($\Delta s_M^{ap,pk}$) with respect to the complete curve one (Δs_M^{pk}). Besides a flat region close to 0 K, there are two values of the initial temperature (T_{ini}^{opt}), for which the Δs_M^{ap} values are coincident with those of the complete curve (marked with arrows in the inset of figure 2). For practical purposes the most useful optimal initial temperature would be the highest, as the necessity to achieve temperatures close to zero is drastically avoided. From now, we focus only on the highest T_{ini}^{opt}. If we consider the relation between the complete entropy, s_H (equation (6) starting from 0 K), and the approximated entropy, s_H^{ap} (equation (6)):

$$s(T) = \int_0^T \frac{c_H}{T} \mathrm{d}T = s_H^{ap}(T) - \frac{1}{2} c_H(T_{\mathrm{ini}}) + \int_0^{T_{\mathrm{ini}}} \frac{c_H}{T} \mathrm{d}T = s_H^{ap}(T) + \xi_H(T_{ini}) \qquad (10)$$

where the parameter ξ_H depends on H and T_{ini}. For any initial temperature, the relation between the approximate magnetic entropy change and the complete one is:

$$\Delta s_M = \Delta s_M^{ap} + [\xi_H(T_{ini}) - \xi_0(T_{ini})] \qquad (11)$$

where the condition for the optimal temperature is:

$$\xi_H\left(T_{ini}^{opt}\right) = \xi_0\left(T_{ini}^{opt}\right) \quad (12)$$

This implies that the shift in the total entropy is the same for both magnetic fields. This condition is equivalent to:

$$\frac{1}{2}\Delta c\left(T_{ini}^{opt}\right) - \int_0^{T_{ini}^{opt}} \frac{\Delta c}{T}\,\mathrm{d}T = 0 \quad (13)$$

with $\Delta c = c_H - c_0$. This constitutes the formal definition of T_{ini}^{opt}. It is worth mentioning that the fulfilment of condition (13) is independent of the model used (Brillouin function in our study).

Figure 3 shows the approximated adiabatic temperature change curves (ΔT_{ad}^{ap}) from different values of the initial temperature of integration using equation (5). Unlike for the Δs_M^{ap} data, the differences with respect to the complete curve are not constant and depend on the temperature. However, as for the Δs_M^{ap} case, it can be observed some initial temperaturevalues for which the differences with respect to the completed curve (integration performed from 0 K)are zero (the differences of the peak of ΔT_{ad}^{ap} with respect to the complete curve are shown in the inset of figure 3). These optimal initial temperatures for ΔT_{ad}^{ap} are the same found for Δs_M^{ap}. To demonstrate this coincidence, we consider the definitions of both ΔT_{ad} and ΔT_{ad}^{ap}:

$$\Delta T_{ad}(T, s) = [T_H(s_H) - T_0(s_0)]_s \quad (14)$$

$$\Delta T_{ad}^{ap}(T, s^{ap}) = [T_H^{ap}\left(s_H^{ap}\right) - T_0^{ap}\left(s_0^{ap}\right)]_{s^{ap}} \quad (15)$$

Where we establish the equality at a certain temperature $T = T_0(s) = T_0^{ap}(s^{ap})$ and from the inverse of equation (10):

$$T_H^{ap}\left(s_H^{ap}\right) = T_H(s_H - \xi_H(T_{ini})) \quad (16)$$

Therefore, as for T_{ini}^{opt} equation (12) holds and the displacements of both approximated curves are the same in the entropy axis with respect to the complete curves, the change

between temperatures remains constant and $\Delta T_{ad}^{ap}(T)=\Delta T_{ad}(T)$. However, when T_{ini} is different to T_{ini}^{opt}, the displacements in entropy axis of the approximated curves differ and the temperature change is not preserved. Figure 4 illustrates the calculus of the different ΔT_{ad}^{ap} values at $T=T_{peak}$: a) shows the procedure when T_{ini}=0 K (corresponding to the complete curve) b) corresponds to $T_{ini}=T_{ini}^{opt}$ (211.5 K) and c) uses T_{ini}=141 K (a value below T_{ini}^{opt}). As observed when $\xi_H(T_{ini}^{opt}) \neq \xi_0(T_{ini}^{opt})$, $\Delta T_{ad}^{ap}(T) \neq \Delta T_{ad}(T)$. Figure 5 shows the $\Delta T_{ad}^{ap}(T)$-$\Delta T_{ad}(T)$ for several initial temperatures at a magnetic field change of 2 T. It can be observed that for a curve with T_{ini} different to T_{ini}^{opt}, the differences with respect to the complete curve increases as temperature increase, while for $T_{ini}=T_{ini}^{opt}$ the differences are zero for all the temperature range. The continuous dependence of $\Delta T_{ad}^{ap}(T_{ini})$-$\Delta T_{ad}(T_{ini})$ is also represented in figure 5 (dotted line) to show the followed trend.

With respect to the field dependence of the analysis, figure 6 shows the field and temperature dependence of $(\Delta s_M^{ap,pk}-\Delta s_M^{pk})/\Delta s_M^{pk}$. It can be observed that the shape of the temperature dependence of this magnitude is not affected by field, although the position of T_{ini}^{opt} is slightly shifted to higher temperatures with increasing field, varying linearly at a rate of 2.1 K/T (inset of figure 5). The shape of the $(\Delta T_{ad}^{ap,pk}-\Delta T_{ad}^{pk})/\Delta T_{ad}^{pk}$ surface is the same. Selecting a single magnetic field (e.g. 1 T that is in the middle of the range explored here) the error using its T_{ini}^{opt} for other magnetic fields is below 1% at the peak, which is within the error margin of the experimental measurements. Using T_{ini} values different to T_{ini}^{opt}, even if they were closer to 0 K than T_{ini}^{opt}, larger errors can be obtained (around 8 % at the peak) and anomalous behaviors in the temperature dependencies of Δs_M and ΔT_{ad} are found (e.g. at the paramagnetic range).

In our simulations, the values of T_{ini}^{opt} mainly depend on the magnetic parameters (J and T_C), while the lattice and electronic parameters (θ_D and γ, respectively) do not show any significant effect. It is worth noting that, fixing T_C for small values of J (1/2 and 1), the curve describing the differences between the approximated calculus and the complete ones does not intercept the $\Delta s_M^{ap,pk}$-Δs_M^{pk}=0 axis, while for higher values of J it does (figure 7). However, if T_C is modified (fixing J>1) the values of T_{ini}^{opt} vary linearly with T_C (inset of figure 7).

3.2 APPLICATION TO EXPERIMENTAL DATA

For practical purposes, the calculus of T_{ini}^{opt} from its mathematical definition in equation (13) is of little use as the complete curves should be known. Nevertheless, as:

1) the previous section demonstrated the existence of T_{ini}^{opt},
2) figure 5 shows that using this starting temperature the approximated curve is corrected for the temperature span starting from T_{ini}^{opt} and
3) both Δs_M and ΔT_{ad} are zero well above the transition temperature,

we can use this property to identify the value of T_{ini}^{opt} for experimental data.

We can focus on the temperature range well above the transition temperature, for which Δs_M and ΔT_{ad} must be practically zero. In this temperature range, the approximated values Δs_M^{ap} and ΔT_{ad}^{ap} should be different to zero (either positive or negative) except for T_{ini}^{opt} (see figures 2 and 3). This feature can be used to identify T_{ini}^{opt} experimentally: T_{ini}^{opt} corresponds to that temperature which produces $\Delta s_M^{ap}(T>>T_C)$ and $\Delta T_{ad}^{ap}(T>>T_C)$=0. The proposed procedure to correct the experimental Δs_M and ΔT_{ad} curves when temperatures close to 0 K were not achievable can be summarized in two simple steps:

1) Calculate the evolution of Δs_M^{ap} and ΔT_{ad}^{ap} curves for different initial temperatures.
2) Find the optimal initial temperature as the value of T_{ini} that makes $\Delta s_M^{ap}=0$ and $\Delta T_{ad}^{ap}=0$ well above the transition (the same optimal initial temperature for both).

The Δs_M^{ap} and ΔT_{ad}^{ap} curves from this optimal initial temperature should be considered as the best approximation (in the range $T> T_{ini}^{opt}$) to the complete curves.

The proposed procedure to minimize the error associated to Δs_M and ΔT_{ad} has been applied to experimental heat capacity data measured for a single phase GdZn material (figure 8). The initial temperature of the measurements is limited by the stability of the grease used in the experimental setup (other greases are suitable to measure at lower temperatures but their range is not extended to room temperature, where the transition occurs). Figure 9 and 10 show the obtained experimental results for Δs_M^{ap} and ΔT_{ad}^{ap}, respectively, calculated using different initial temperatures. It can be observed that ~100 K above the peak temperature (where Δs_M^{ap} curves remain almost constant), the values of Δs_M^{ap} and ΔT_{ad}^{ap} reach zero only for a $T_{ini}^{opt}\approx$221.5 K (as predicted, the temperature is coincident for Δs_M and ΔT_{ad} data). Moreover, the behavior of the curves is in agreement with the predictions derived from our simulations: while Δs_M varies due to T_{ini} as a temperature independent shift, the ΔT_{ad} varies in a more complex form (changing with temperature).

In order to confirm the validity of the procedure proposed here, we have compared the obtained optimal Δs_M^{ap} and ΔT_{ad}^{ap} curves to calculations from independent magnetization measurements (hollow symbols in figures 9 and 10) using equations (1) and (2), respectively. An excellent agreement between both procedures can be observed.

It is worth mentioning that, using the procedure proposed in this work, measurements at low temperatures are not needed and we avoid the necessity to combine two types of measurements (that requires a careful sample preparation to avoid artefacts in the different measurements and a large number of measurements as a function of *H* and *T* for both magnetization and heat capacity data).

4. CONCLUSIONS

We propose a procedure to minimize the associated error in the approximated calculus of the magnetocaloric parameters from heat capacity measurements. It is based on the existence of optimal initial temperatures that correct the effect of truncation of the temperature integration range (as temperatures close to 0 K can be beyond the experimental range). The optimal initial temperatures are found to be the same for Δs_M and ΔT_{ad} data. These optimal temperatures can be found as the initial temperatures that make the calculated Δs_M and ΔT_{ad} zero well above the transition. These features have been checked through numerical simulations and experimental measurements in a single phase GdZn alloys. A good agreement has been found between the results using the present procedure and those data obtained using the combination of heat capacity and magnetization measurements.

ACKNOWLEDGEMENTS

This work was supported by the Spanish MINECO (project MAT2013-45165-P) and the PAI of the Regional Government of Andalucía. L.M. Moreno-Ramírez acknowledges a FPU fellowship from the Spanish MECD.

FIGURES

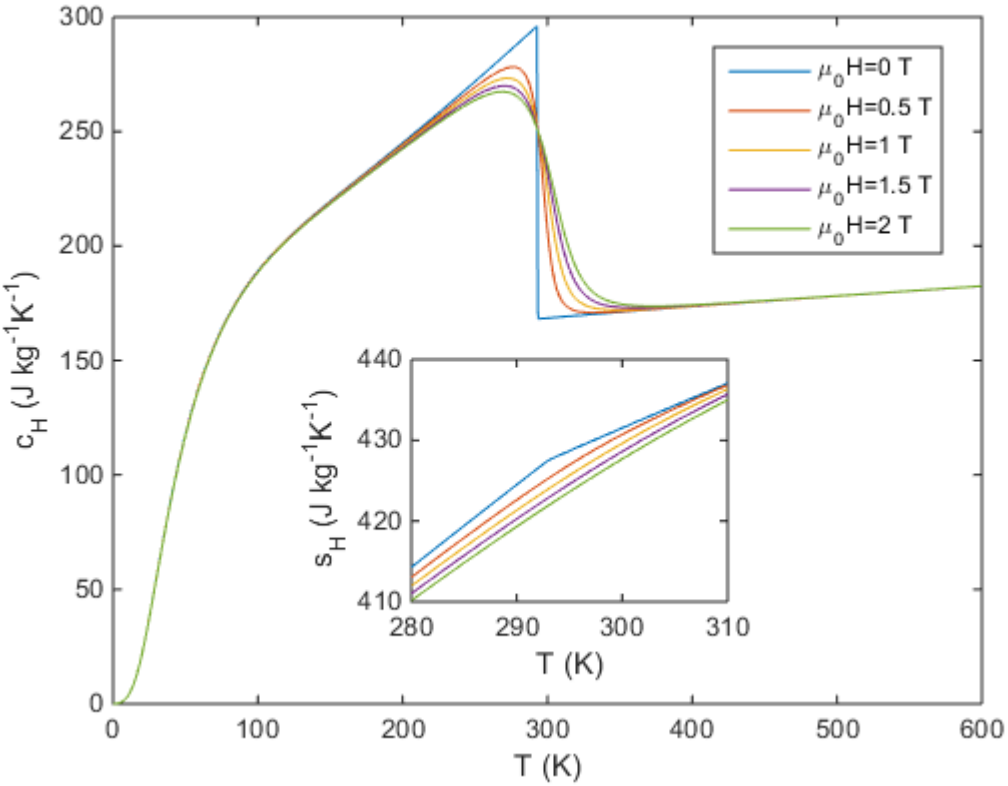

Figure 1. Simulated specific heat capacity data from 0 K for different magnetic fields. Inset: Specific total entropy obtained using simulated c_H data.

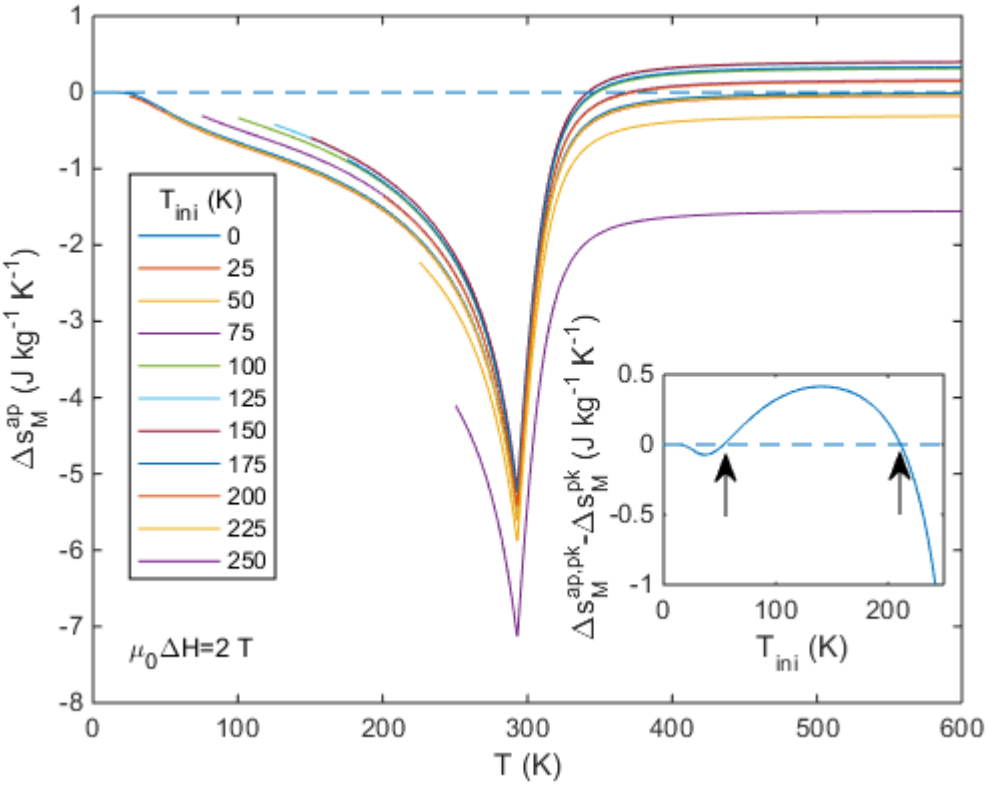

Figure 2. Approximated specific magnetic entropy change for a magnetic field change of 2 T for different initial temperatures. Inset: Differences between the peak values of $\Delta s_M{}^{ap}$ for each T_{ini} with respect to the peak value with T_{ini}=0 K. T_{ini}^{opt} values are marked with arrows.

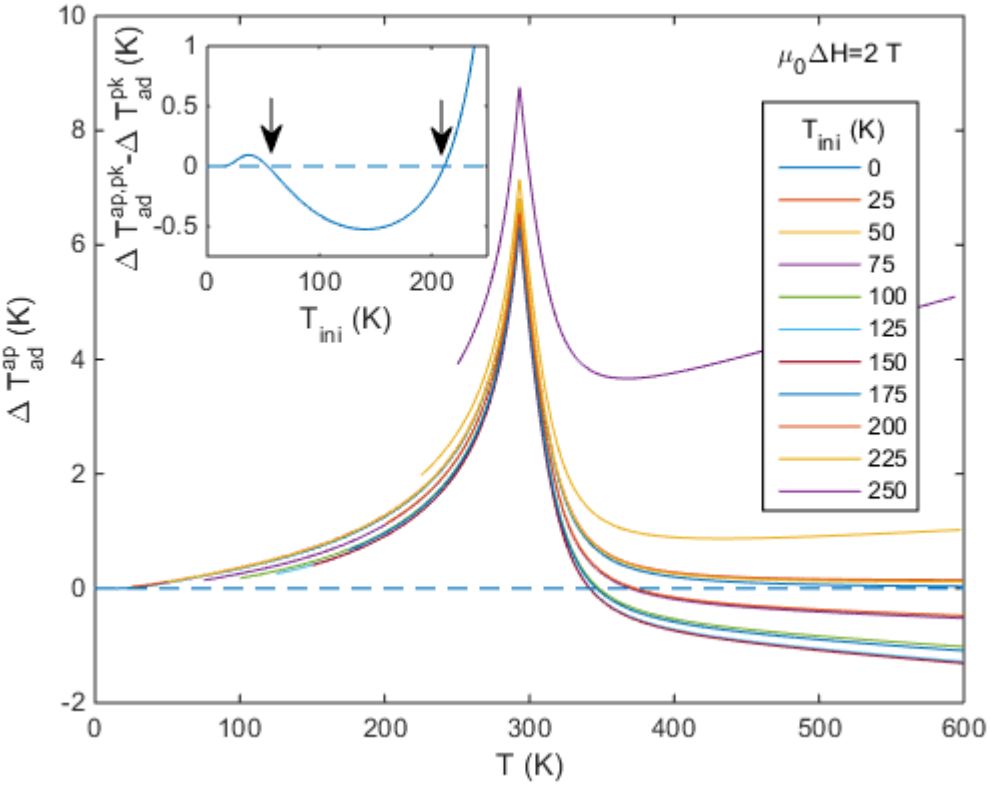

Figure 3. Approximated adiabatic temperature change for a magnetic field change of 2 T for different initial temperatures. Inset: Differences between the peak values of ΔT_{ad}^{ap} for each T_{ini} with respect to the peak value with T_{ini}=0 K. T_{ini}^{opt} values are marked with arrows.

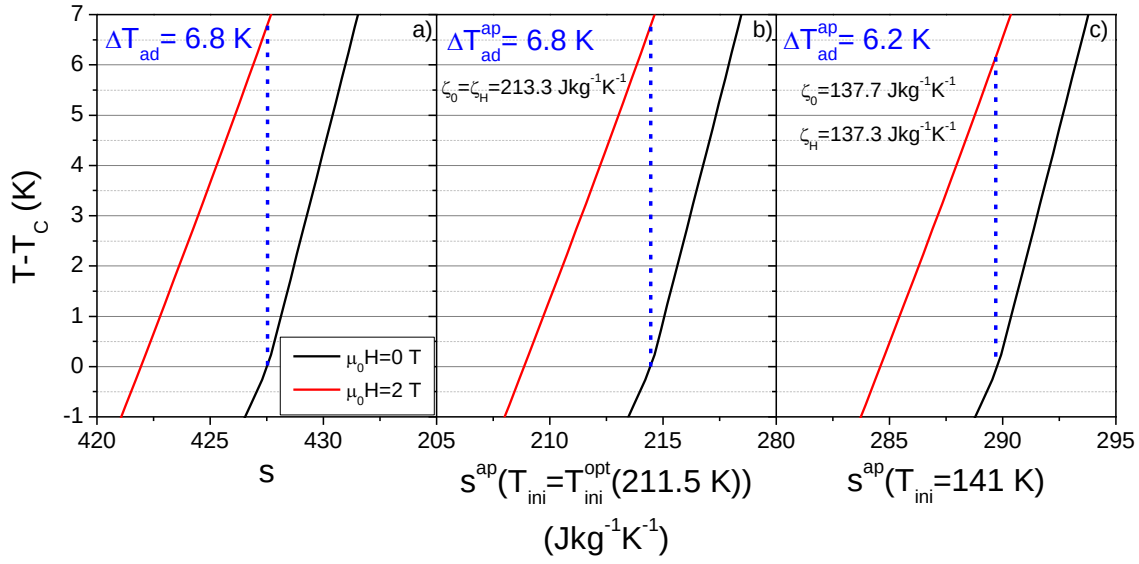

Figure 4. Illustration of the procedure to obtain the adiabatic temperature change from

temperature versus entropy curves for: a) T_{ini}=0 K b) T_{ini}=T_{ini}^{opt} (211.5 K) and c) T_{ini}=141 K.

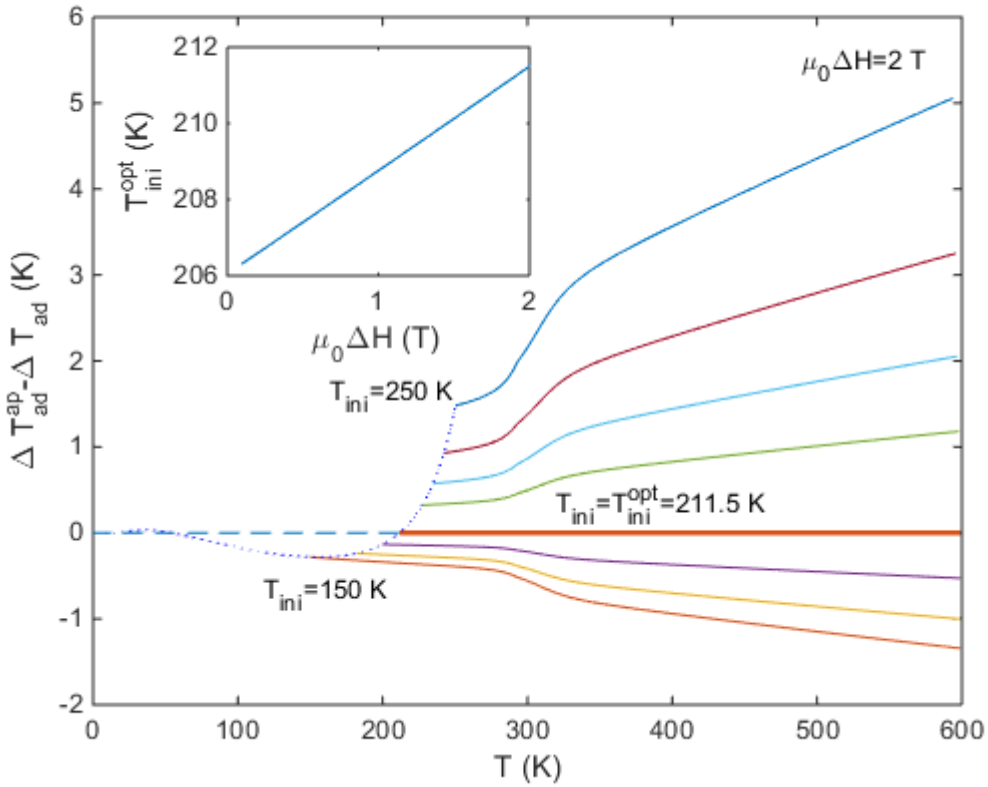

Figure 5. ΔT_{ad}^{ap}-ΔT_{ad} curves for different initial temperatures in all the temperature range above the corresponding T_{ini}. Dotted line represents this differences at T_{ini} in a continuous curve. Inset: T_{ini}^{opt} for different magnetic field change.

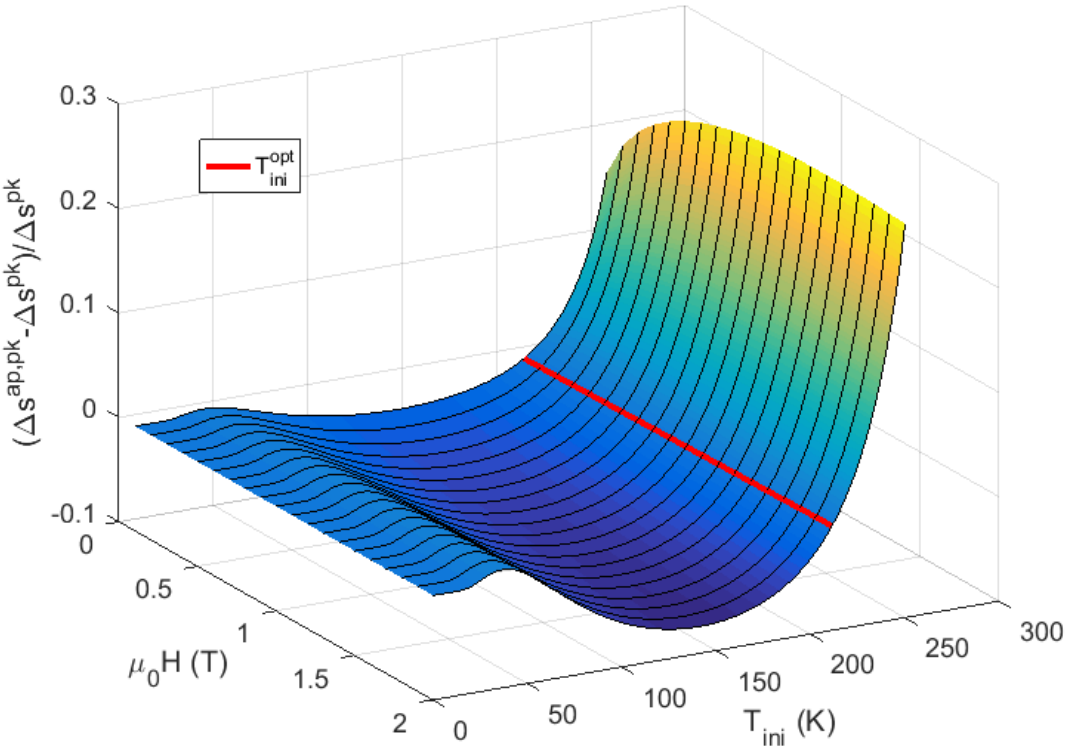

Figure 6. Field and temperature dependence of $(\Delta s_M^{ap,pk}-\Delta s_M^{pk})/\Delta s_M^{pk}$. The red line corresponds to the T_{ini}^{opt} values as a function of the magnetic field.

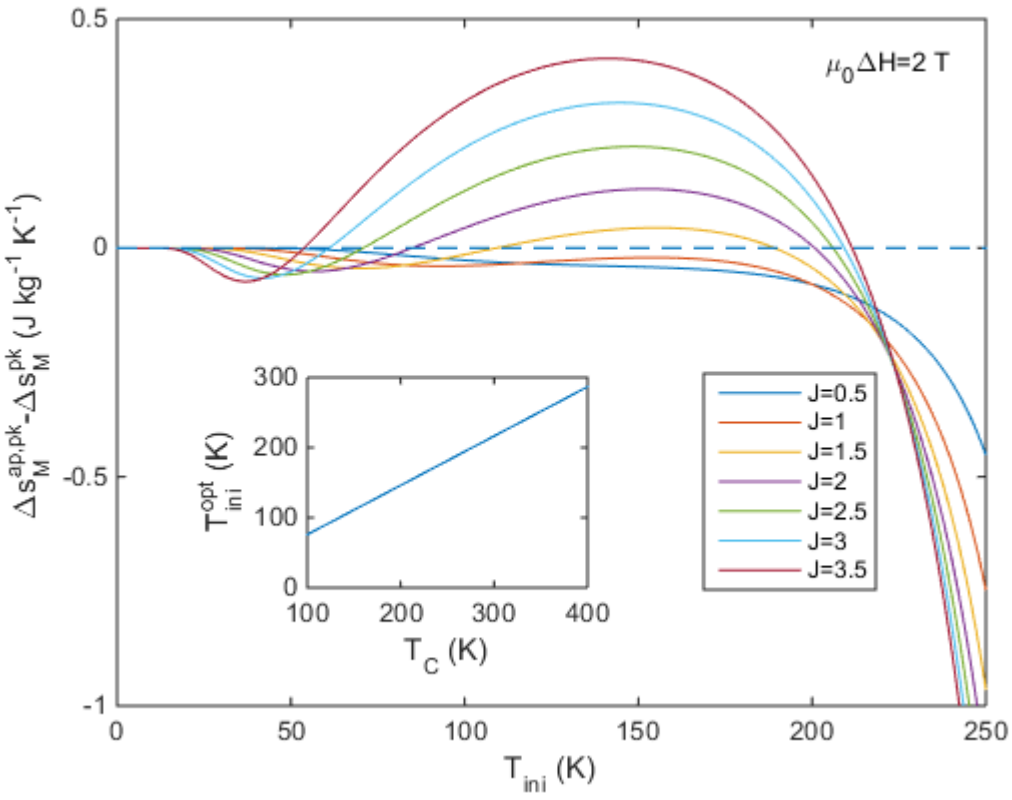

Figure 7. Differences between the peak value of Δs_M^{ap} at a T_{ini} with respect to the peak value from T_{ini}=0 K for different J values (T_C=293 K). Inset: T_{ini}^{opt} as a function of T_C for J=3.5.

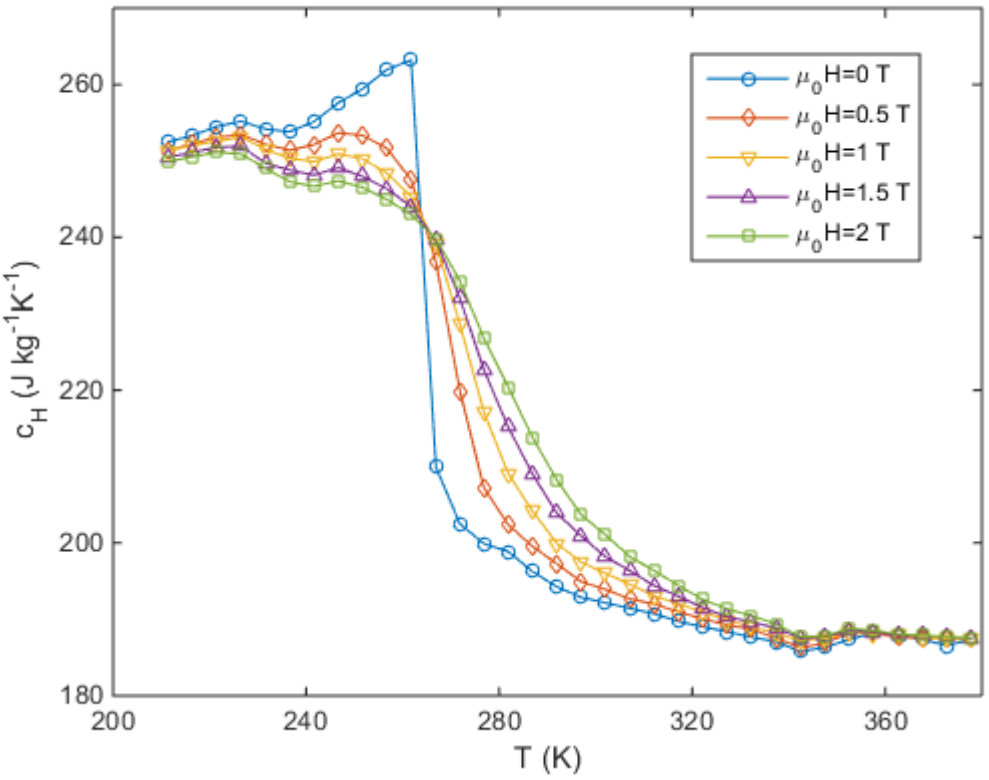

Figure 8. Experimental specific heat capacity data for a GdZn alloy for different magnetic fields.

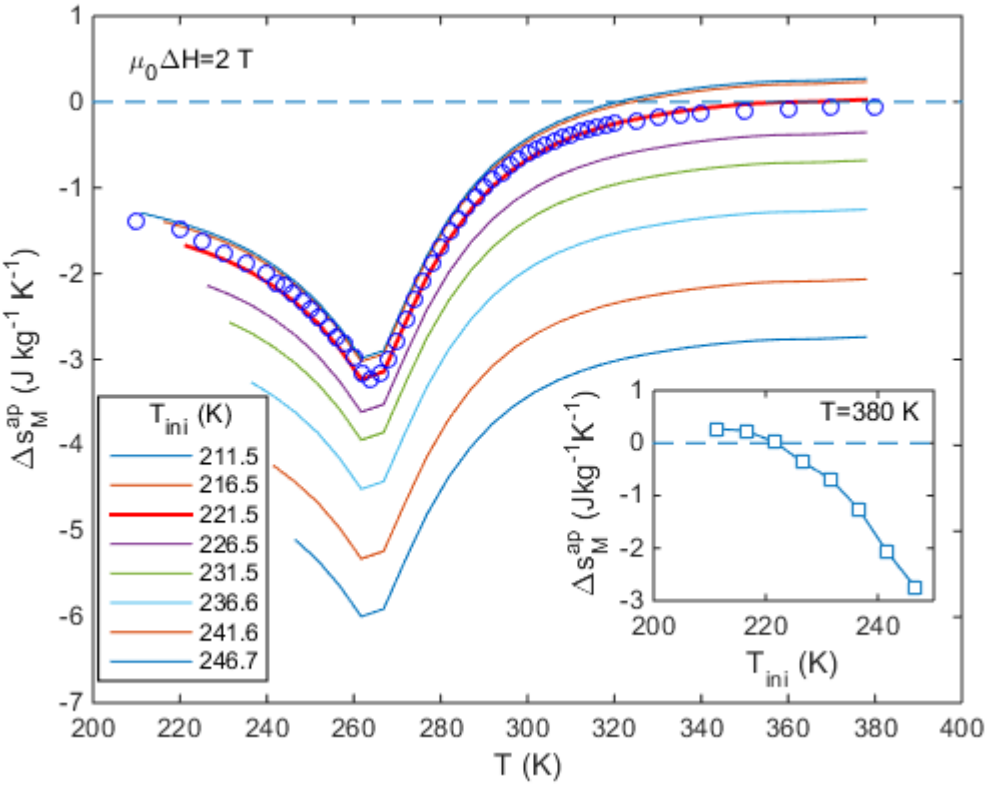

Figure 9. Calculated Δs_M^{ap} values from experimental heat capacity data for a GdZn alloy using different initial temperatures at $\mu_0\Delta H$=2 T. Circles represents the experimental values derived from magnetization measurements and obtained using equation (3). Inset: Evolution of Δs_M^{ap} well above T_C for different T_{ini}. The intercept of this curve with zero is used to find T_{ini}^{opt} (marked with an arrow).

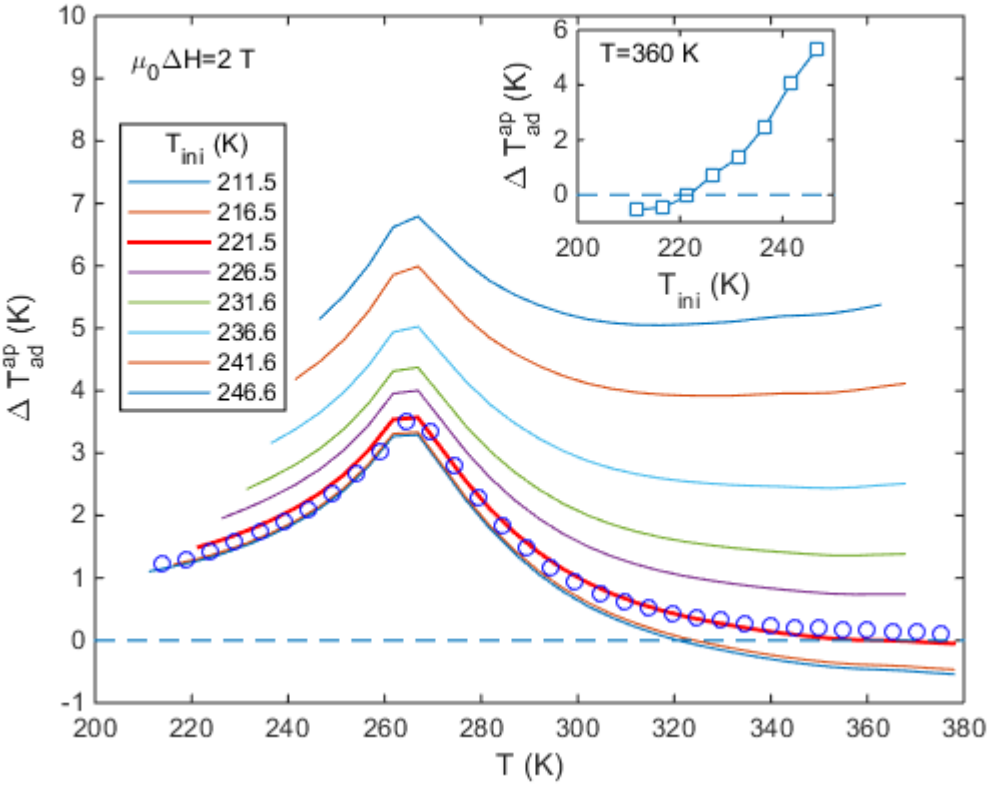

Figure 10. Calculated ΔT_{ad}^{ap} values from experimental heat capacity data for a GdZn alloy for different initial temperatures at $\mu_0\Delta H$=2 T. Circles represents the experimental values from combining magnetization and calorimetric data and obtained using equation (5). Inset: Evolution of ΔT_{ad}^{ap} well above T_C for different T_{ini}. The intercept of this curve with zero is used to find T_{ini}^{opt} (marked with an arrow).

[1] A.M. Tishin, Y.I. Spichkin, The magnetocaloric effect and its applications, Institute of Physics Publishing (2003).
[2] E. Brück, J. Phys. D: Appl. Phys. 38, R381–R391 (2005)
[3] W.F. Giauque, D.P. MacDougall. Phys. Rev. 43 (1933) 768.
[4] V. Franco, J. S. Blázquez, B. Ingale, A. Conde, Annu. Rev. Mater. Res. 42, 305-342 (2012).
[5] O. Gutfleish, M.A. Willard, E. Brück, C.H. Chen, S.G. Sankar, J. P. Liu, Advanced Materials, 23, 821-842 (2011)
[6] H.B. Callen, Thermodynamics and an Introduction to Thermostatistics, 2ND edition, John Wiley & Sons (1985).
[7] V.K. Pecharsky, K.A. Gschneidner, J. Appl. Phys. 86, 565-575 (1999).
[8] G. Wang, E. Palacios, A.A. Coelho, S. Gama, R. Burriel, EPJ Web of conferences 75, 04003 (2014).
[9] C. Kittel, Introduction to Solid State Physics ISBN 978-0471415268
[10] J.S. Smart, *Effective field theories of magnetism*, Philadelphia, London: W. B. Saunders (1966)
[11] R. W. Hill, S. J. Collocott, K. A. Gschneidner, Jr., and F. A. Schmidt, J. Phys. F: Met. Phys. 17, 1867–1884 (1987).
[12] J.Y. Law, L.M. Moreno-Ramírez, J.S. Blázquez, V. Franco, A. Conde, J. All. Compd. 675, 244–247 (2016)
[13] R. E. Camley, Phys. Rev. B. 35, 3608-3611 (1987).
[14] A. Berger, A. W. Pang, and H. Hopster, Phys. Rev. B 52, 1078 (1995)
[15] S. Y. Dan'kov, A. M. Tishin, V. K. Pecharsky, K. A. Gschneidner, Phys. Rev. B 57, 3478-3490 (1998)